Available online at www.sciencedirect.com
SCIENCE DIRECT®
Agricultural and Forest Meteorology 130 (2005) 176–192
AGRICULTURAL AND FOREST METEOROLOGY
www.elsevier.com/locate/agrformet

Relationship between soil CO_2 concentrations and forest-floor CO_2 effluxes

Rachhpal Jassal *, Andy Black, Mike Novak, Kai Morgenstern, Zoran Nesic, David Gaumont-Guay

Faculty of Agricultural Sciences, University of British Columbia, Vancouver, BC, Canada V6T 1Z4

Received 19 November 2004; accepted 8 March 2005

Abstract

To better understand the biotic and abiotic factors that control soil CO_2 efflux, we compared seasonal and diurnal variations in simultaneously measured forest-floor CO_2 effluxes and soil CO_2 concentration profiles in a 54-year-old Douglas fir forest on the east coast of Vancouver Island. We used small solid-state infrared CO_2 sensors for long-term continuous real-time measurement of CO_2 concentrations at different depths, and measured half-hourly soil CO_2 effluxes with an automated non-steady-state chamber. We describe a simple steady-state method to measure CO_2 diffusivity in undisturbed soil cores. The method accounts for the CO_2 production in the soil and uses an analytical solution to the diffusion equation. The diffusivity was related to air-filled porosity by a power law function, which was independent of soil depth. CO_2 concentration at all depths increased with increase in soil temperature, likely due to a rise in CO_2 production, and with increase in soil water content due to decreased diffusivity or increased CO_2 production or both. It also increased with soil depth reaching almost 10 mmol mol^{-1} at the 50-cm depth. Annually, soil CO_2 efflux was best described by an exponential function of soil temperature at the 5-cm depth, with the reference efflux at 10 °C (F_{10}) of 2.6 μmol m^{-2} s^{-1} and the Q_{10} of 3.7. No evidence of displacement of CO_2-rich soil air with rain was observed.

Effluxes calculated from soil CO_2 concentration gradients near the surface closely agreed with the measured effluxes. Calculations indicated that more than 75% of the soil CO_2 efflux originated in the top 20 cm soil. Calculated CO_2 production varied with soil temperature, soil water content and season, and when scaled to 10 °C also showed some diurnal variation. Soil CO_2 efflux and concentrations as well as soil temperature at the 5-cm depth varied in phase. Changes in CO_2 storage in the 0–50 cm soil layer were an order of magnitude smaller than measured effluxes. Soil CO_2 efflux was proportional to CO_2 concentration at the 50-cm depth with the slope determined by soil water content, which was consistent with a simple steady-state analytical model of diffusive transport of CO_2 in the soil. The latter proved successful in calculating effluxes during 2004.

Keywords: Soil CO_2 efflux; Soil CO_2 concentration; Diffusivity measurement; Soil CO_2 production profile; Steady-state diffusion model

* Corresponding author.
E-mail address: rachhpal.jassal@ubc.ca (R. Jassal).

0168-1923/$ – see front matter
doi:10.1016/j.agrformet.2005.03.005

1. Introduction

Worldwide concern with global climate change and its effects on our future environment requires a better understanding of the global carbon cycle. Soils are of particular importance in the global carbon cycle (Houghton et al., 1995; Schimel, 1995) as they contain more carbon than live biomass (Eswaran et al., 1993), and the emission of CO_2 from the soil is a major flux of C into the atmosphere (Schlesinger and Andrews, 2000). Soil CO_2 efflux represents 40–80% of forest ecosystem respiration (Janssens et al., 2001; Law et al., 1999) and is, therefore, one of the major processes to consider when determining the carbon balance of forests.

Over the last decade, research has focussed on the measurement of fluxes at the soil surface using a variety of chamber and micrometeorological methods. However, there is considerably less information available on CO_2 dynamics below the soil surface, apparently due to the difficulty of sampling and measuring soil CO_2 concentrations. Though process-based models (e.g. Fang and Moncrieff, 1999; Jassal et al., 2004; Simunek and Saurez, 1993) are valuable tools in increasing our understanding of various processes governing the CO_2 exchange within the soil, they need to be validated using measurements.

In a limited number of studies on the measurement of soil CO_2 concentrations, samples are either extracted using syringes from gas sampling tubes (e.g. Davidson and Trumbore, 1995; Drewitt et al., 2005), which have been installed in the soil at different depths, or withdrawn by a pump (e.g. Fang and Moncrieff, 1998; Hirsch et al., 2002). Such sampling, however, causes disturbance to the soil environment, and can, therefore, lead to bias in the measurements. Also, such sampling techniques are not suited to the continuous monitoring of soil CO_2 concentrations needed to investigate diurnal changes in CO_2 storage in the soil. Recently, fast response, industrial solid-state sensors that can be used to measure soil CO_2 concentrations have become available. Liang et al. (2004) and Tang et al. (2003) reported continuous measurements of soil CO_2 concentrations with such sensors buried in a Japanese larch forest and a relatively dry silt loam soil in a Mediterranean savanna ecosystem in California, respectively. We adapted, calibrated and tested similar solid-state sensors to continuously measure CO_2 concentrations in a relatively wet temperate forest ecosystem soil in British Columbia, Canada (Jassal et al., 2004).

Emission of CO_2 from soil is the result of CO_2 production in the soil and its transport to the surface. Under most field soil conditions, when changes in barometric pressure are small, transport of gases in the soil is mainly by diffusion in air-filled pores. But our understanding of production and transport of CO_2 in soil and how these processes are affected by changes in meteorological and soil variables is poor. Production of CO_2 in soil is the result of microbial (heterotrophic) and root (autotrophic) respiration. These are functions of the type and distribution of organic matter and roots in soil, respectively, and are governed by mainly soil temperature and water content. Soil CO_2 diffusivity changes with air-filled porosity, which in turn is affected by soil bulk density and soil water content. Soil temperature also affects diffusivity. Thus, both the soil CO_2 efflux and soil CO_2 concentrations are regulated by the production and transport of CO_2 in the soil and are, therefore, interdependent. The first objective of this paper is to study diurnal and seasonal variations in long-term continuously measured belowground soil CO_2 concentrations and simultaneously measured forest-floor CO_2 effluxes, and examine relationships between the two. Simulations with a process-based model (Jassal et al., 2004) showed that in a rapidly draining soil at the same site as in this study, the CO_2 efflux, at time scales as low as 30 min, appeared to be well approximated by the rate of total CO_2 production in the soil profile, i.e. near steady-state conditions. This was attributed to relatively rapid CO_2 diffusion compared to changes in the rate of CO_2 production. The second objective of this study is to confirm these results and examine the applicability of a simple steady-state model to calculate the efflux from measurements of soil CO_2 concentration.

2. Materials and methods

2.1. Site description and soil characteristics

Measurements were made during 2003 in a 54-year-old Douglas-fir stand located about 10 km southwest of Campbell River (49°51′ N, 125°19′ W,

300 m above mean sea level), on the east coast of Vancouver Island, Canada. The site naturally regenerated after a forest fire in 1949 resulting in an almost homogeneous stand. Tree density was about 1100 stems ha^{-1}, tree height was about 33 m, and mean tree diameter at the 1.3 m height was 29 cm. The aboveground estimate of organic carbon (OC) was about 19 kg m^{-2} ground surface area.

The soil is a humo-ferric podzol underlain by glacial till at a depth of 1 m and a variable surface organic layer of 0–6 cm thick, with mineral soil below the organic layer varying from gravelly loamy sand in the 0–40 cm layer to sandy loam below the 40-cm depth (Drewitt et al., 2002). We selected a location that was relatively level, uniform and free of large stones. Bulk density at the location of the experiment varied from 1050 kg m^{-3} in the 0–10 cm layer to 1500 kg m^{-3} at the 50-cm depth, while the coarse fragments varied from 11% in the 0–10 cm layer to 5% in the 40–50 cm layer with majority of the coarse faction particles being <15 mm diameter. The top 1 m of the mineral soil contained 11.6 kg OC m^{-2}, which with 2.3 kg m^{-2} in the roots and 3 kg m^{-2} in the surface organic layer resulted in a total of 16.9 kg m^{-2} of belowground OC.

Half-hourly measurements of soil water content and soil temperature profiles were made continuously. Soil volumetric water content was measured using four CSI water content reflectometers (model CS-615, Campbell Scientific Inc., Logan, UT, USA) at the 1–2, 10–12, 35–48 and 70–100-cm depths, and corrected for the coarse fraction. Soil temperature measurements were made at the 5-, 10-, 20-, and 50-cm depths with copper-constantan thermocouples at the location of CO_2 efflux and concentration measurements, which were located about 5 m from the CS-615 probes.

The sign conventions followed in this paper are: CO_2 flux in the soil and at the soil surface, i.e. efflux, are positive upward, distance below the soil surface is negative (Jury et al., 1991), and soil CO_2 production is positive.

2.2. Measurement of soil CO_2 diffusivity on undisturbed soil cores

Soil cores, 10 cm long with an internal diameter of 11 cm, were excavated from 0 to 10, 10 to 20, 20 to 30, 30 to 40 and 40 to 50 cm soil depths at three locations within a radius of 5 m from the location of efflux and concentration measurements. The three profiles showed little spatial variability. The cores were brought into the laboratory under high soil water content. To make diffusivity measurements at a range of soil water contents, soil cores were subjected to two episodes of drying with no wetting in between the measurements. For drying, soil cores were placed under a fan for up to 2 days, then wrapped in polyethylene sheet and stored at room temperature for 2–4 weeks to redistribute the soil water content. Air-filled porosity calculations were made using total bulk density.

Gas diffusivity of undisturbed soil cores was measured in the laboratory under steady-state conditions using CO_2 as the diffusing gas. The method involved maintaining a high (~9 mmol mol^{-1}) constant concentration at the lower end (CD) of the soil column by passing the gas through a 800-cm^3 chamber attached to the lower end while the upper end (AB) was exposed to atmospheric ambient concentration (~390 μmol mol^{-1}) (Fig. 1). CO_2 diffusivity was calculated using $D = L\ (F_0 - F_S/2)/(C_L - C_0)$ (see Appendix A), where F_0 is the soil CO_2 efflux at the upper end of the column, $(C_L - C_0)$ is the concentration difference across the soil column of length L

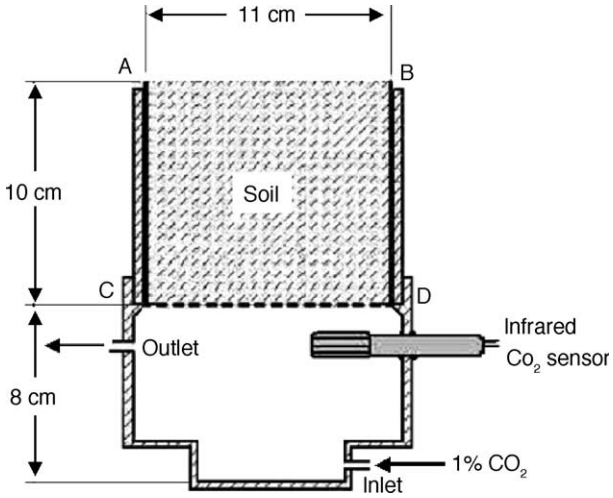

Fig. 1. A schematic diagram showing the apparatus used for measurement of diffusivity of undisturbed 11-cm diameter soil cores. The efflux was measured by placing a 1.5 dm^3 chamber over the surface AB and measuring the rate of increase in CO_2 concentration in the chamber over 2-min periods.

(=10 cm in Fig. 1), and $F_S/2$ is the correction for CO_2 production in the soil column. The corrections were 10 and 3% of the measured efflux for cores from the top 10 cm and deeper in the soil, respectively. CO_2 production (F_S) was determined by sealing the lower end of each soil column and measuring the efflux at the upper end as described below.

A Vaisala infrared CO_2 sensor (model GMM221, Vaisala Oyj, Helsinki, Finland, see Section 2.3) was used to measure the concentration in the lower gas chamber. Before use, the sensor was calibrated against an infrared gas analyser (IRGA) (model LI-820, LI-COR Inc., Lincoln, NE, USA) as explained in the next section. The sensor was inserted into the lower chamber and connected to a CR-21X data logger, which was programmed to excite the sensor for the first 4 min of each 6-min interval in order to eliminate any temperature increase in the lower chamber due to sensor heating. The constant high concentration of CO_2 in the lower chamber was established by flushing with 1% CO_2 in dry air. The CO_2 efflux at the surface was obtained by measuring the rate of increase of CO_2 concentration during the last 2 min of the excitation period by placing a 1.5-dm^3 (1 dm^3 = 1 L) chamber over the upper end, AB (Fig. 1) of the soil column. This was repeated five to six times after steady-state conditions were established, which took nearly 1 h to achieve. Air was circulated through the chamber and the LI-820 IRGA using a small diaphragm pump (model TD-4X2N, Brailsford Co., NY, USA). A Vaisala HMP 35-C Humicap humidity sensor (and thermistor) was used to measure water vapour concentration in the sample air to correct the CO_2 efflux for dilution effects. Care was taken while placing the sampling chamber over the soil column to avoid creating static pressure differences across the two ends of the soil column, which could result in pressure pumping, i.e. losses by mass flow. Widen and Lindroth (2003) reported that a pressure difference as small as 0.15 Pa resulted in an 11–40% error in the measured efflux, depending on air-filled porosity. We observed that the measured efflux increased with an increase in flow rate of the gas through the lower chamber. This was attributed to development of a static pressure difference across the soil column. The pressure difference was monitored at a frequency of 2 Hz with a differential pressure transducer (model Omega PX 653, Omega Engineering Inc., Stanford, CT, USA). It was found that a flow rate of 40 cm^3 min^{-1} through the lower chamber resulted in sufficiently low ($\pm$0.05 Pa) pressure differences while still maintaining a constant concentration of about 8200–9200 $\mu mol\ mol^{-1}$ in the chamber. The range of this concentration depended on gas flow characteristics of the soil column. Furthermore, it was found that blowing water-saturated air across the soil surface to prevent moisture loss from the soil during measurements increased effluxes. This was attributed to increased turbulence in the boundary layer at the surface (Widen and Lindroth, 2003). Therefore, this procedure was not used and the soil surface was exposed to ambient air conditions in the laboratory. However, weighing the soil cores before and after efflux measurements showed that there was negligible change ($\leq$0.001 m^3 m^{-3}) in soil water content during the 30-min measurement period for each core. We also occasionally measured the CO_2 concentrations at the soil surface by drawing samples with horizontally placed tubing, and attributed the variation of 390 ± 17 $\mu mol\ mol^{-1}$ to normal conditions in the laboratory.

2.3. Field measurement of soil CO_2 concentrations

Soil CO_2 concentrations at the 10-, 20- and 50-cm depths were continuously measured, from 15 March 2004 to 30 December 2004, with GMM221 CO_2 sensors. The sensor is 10 cm long, 2 cm in diameter and has a time constant of 20 s. Because their zero offsets and sensitivities differed, we calibrated all the sensors before use in the field at concentrations up to 20 $mmol\ mol^{-1}$ against an LI-820 IRGA using a 7.5-cm-long optical bench. For this purpose, the sensors were inserted in a 10-dm^3 container in which air at $\sim$20 $mmol\ mol^{-1}$ CO_2 was continuously mixed with a fan and simultaneously circulated through the IRGA. The container was provided with a small leak to allow slow decrease in the CO_2 concentration in the container with time. We also determined the sensitivity of the CO_2 sensors to changes in temperature and relative humidity at a constant CO_2 concentration of 10 $mmol\ mol^{-1}$. Temperature sensitivity was measured, at two relative humidities, 30 and 80%, by inserting the probe into a column of 70–100 mesh glass beads, initially at 2 °C, and passing 10 $mmol\ mol^{-1}$ CO_2 gas through the column, as the

column warmed by exposure to ambient air. The measured CO_2 concentrations decreased as the temperature increased from 3 to 21 °C, irrespective of relative humidity, giving temperature coefficients of -45 ± 15 μmol mol^{-1} K^{-1} for different sensors, compared to -30 μmol mol^{-1} K^{-1} (-0.1% of full scale K^{-1}) reported by the manufacturer. There was no effect on the measurements when the relative humidity was increased from 15 to 98% in controlled laboratory experiments.

The sensors were inserted into horizontal holes made by augering into the face of a pit, which was carefully back-filled layer-wise to minimize the disturbance. Before installation, the sensors were covered with microporous Teflon tubing (to avoid possible wetting during rainfall events) and excited for only 5 min during each hour (to avoid localized heating) as explained in Jassal et al. (2004). Microporous Teflon tubing excludes water but allows free gas exchange. Soil temperatures were measured using copper-constantan thermocouples inserted at the same depths as the CO_2 sensors but at a lateral distance of 10 cm away from the probes. As the CO_2 sensors were calibrated in the laboratory at 20 °C, all measurements were corrected based on the temperature coefficients of the respective sensors.

2.4. Field measurement of soil CO_2 effluxes

Half-hourly soil CO_2 efflux measurements were made beginning on 15 June 2003 at the soil surface exactly above the location of the CO_2 probes described above, using a dynamic closed (i.e. non-steady-state) automated chamber. The automated chamber consisted of a PVC cylinder and a transparent Plexiglas dome that was fitted to the cylinder with a hinged aluminium frame. The PVC cylinder dimensions were 52.5 cm internal diameter, 13 cm height, and 1 cm thickness while the nearly hemi-spherical dome had a height of 20.5 cm. A foam gasket attached to a horizontal flange at the base of the dome provided a good seal when the chamber was closed. The cylinder was inserted to a depth of about 2 cm below the soil surface. When closed, the chamber headspace volume, V, was 56 dm^3 while the soil surface area covered by the chamber, A, was 0.216 m^2. The opening and closing of the dome was controlled by a two-way pneumatic cylinder (model BFT-173-DN, Bimba Manufacturing Co., Monee, IL, USA) operated by compressed dry air, the release of which was controlled by a solenoid valve (model 45A-AA1-DAA-1BA, Mac Valves Inc., Wixom, MI, USA). The CO_2 sampling, analysis, and the system control unit were housed in an insulated box and consisted of an LI-820 IRGA, a Campbell Scientific 21X data logger, an AC linear pump (model SPP-40GBLS-101, GAST Manufacturing Corp., Benton Harbor, MI, USA) with necessary plumbing and two electronic relays to control the switching on and off of the chamber and the pump.

Effects of fluctuations in atmospheric pressure, which are known to influence fluxes (Kanemasu et al., 1974; Widen and Lindroth, 2003), were avoided by providing a vent consisting of a 15 cm length of 3 mm i.d. Synflex 1300 tubing (Saint-Gobain Performance Plastics, Wayne, NJ) in the dome. Calibration and evaluation of system accuracy were performed in the laboratory by injecting into the dome a small known amount of high CO_2 concentration gas using a mass flow controller (model 1179, MKS Instruments, Andover, MA, USA), and measuring the apparent flux. The effective volume was approximately 10% higher than the geometric headspace-volume, mainly due to adsorption of CO_2 on the chamber material.

CO_2 concentration in the chamber headspace was measured by circulating air at a flow rate of 15 dm^3 min^{-1} between the chamber headspace and the IRGA. While a high pumping rate was necessary to achieve good mixing in the headspace volume, only 700 cm^3 min^{-1} was passed through the gas analyser, with the rest flowing through a bypass. The system was programmed to switch on the pump at the beginning of a 30-min period, close the chamber at 1 min after the pump started and open it 3 min later, and to switch the pump off at 5 min. The time rate of change in CO_2 mole fraction in the chamber headspace (dC/dt, mol mol^{-1} s^{-1}) during 100 s starting 30 s after the closing of the chamber, which was found to be linear, was used to calculate the efflux, F_e (mol m^{-2} s^{-1}) using:

$$F_e = \frac{aPV}{ART}\frac{dC}{dt} \quad (1)$$

where P is the atmospheric pressure (Pa), R is the universal gas constant (8.314 J mol^{-1} K^{-1}), T is the temperature of chamber air (K) and a is the ratio of the

effective volume to the geometric volume of the chamber (1.1). The correction factor, a (Goulden and Crill, 1997; Drewitt et al., 2002), accounts for loss of CO_2 from the chamber headspace during the measurements, mainly due to adsorption on the chamber walls and partly due to leaks through the chamber gasket and diffusion through the vent tube. The measurements from 10 s before to 10 s after the start of the lid closure were assumed to provide ambient CO_2 concentration at the ground level. The IRGA was calibrated at the site every 2–4 weeks. With very low evaporation rates from the forest-floor (a maximum of 0.4 mm/day), calculations showed that water vapour dilution effects on CO_2 efflux (Welles et al., 2001) were less than 1%, and were, therefore, not considered.

3. Results and discussion

3.1. Soil CO_2 diffusivities

Soil CO_2 flux, F and concentration, C are related through effective diffusivity, D as:

$$F = -D\frac{\partial C}{\partial z} \quad (2)$$

where $D = D_m \varepsilon \tau$, in which D_m is the molecular diffusivity of CO_2 in air, ε is the soil air-filled porosity and τ is the tortuosity accounting for the zigzag path length through the soil air pores. The product $\varepsilon\tau$ ($=D/D_m$) has been defined as the tortuosity factor, ξ (Jury et al., 1991) and is normally studied as a function of ε (Rolston, 1986). Penman (1940) proposed a linear relationship between ξ and ε, while Marshall (1959) found that ξ was given by $\varepsilon^{1.5}$. Millington (1959) and Millington and Quirk (1961) derived $\xi = \varepsilon^{10/3}/\theta_s^2$, based on the area of the pore space available for flow and probability of the continuity of pores within an isotropic porous media, where θ_s is the total soil porosity. Currie (1965) studied gas diffusivities in different porous media and found a non-linear relation, $\xi = n\varepsilon^m$, where the constants n and m were determined empirically. Moldrup et al. (1999) considered the soil type effect and proposed $\xi = \varepsilon^{2+3/b}/\theta_s^{3/b}$, where b is the Clapp and Hornberger parameter relating soil water content and matric potential. Fig. 2 shows a comparison of our measurements with estimates using the Penman (1940), Marshall (1959), Millington and Quirk (1961) and Moldrup et al. (1999) relationships. All of these models agree well at high ε while the Penman and Marshall models over-estimate diffusivities and the Millington–Quirk and Moldrup models under-estimate diffusivities at very low ε. Similar results have been reported by Sallam et al. (1984), though the Millington–Quirk model has been found to give fairly accurate estimates of gas diffusivities at very low ε (Sallam et al., 1984; Petersen et al., 1994). The value of b used in these calculations was 1.7 (Jassal et al., 2004). Our measurements were best described by:

$$\xi = 1.18\varepsilon^{2.27} \quad (3)$$

This relationship was independent of soil depth (Fig. 2).

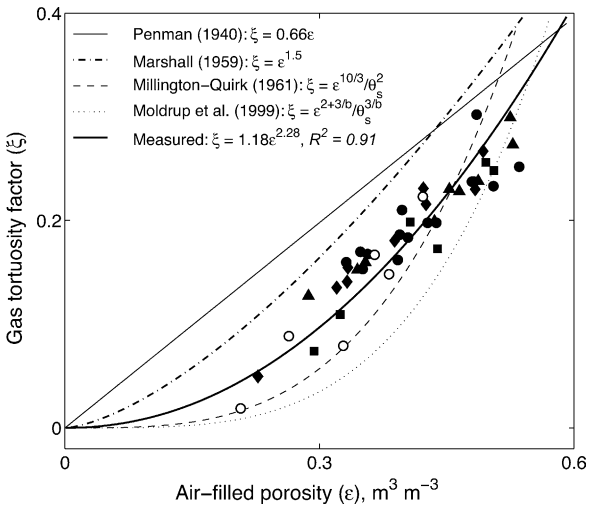

Fig. 2. Effect of soil air-filled porosity on the measured gas tortuosity factor (diffusivity relative to that for still air), and comparison with values calculated using some published models. Symbols distinguish measurements on soil cores from different depths: solid circles 0–10 cm, triangles 10–20 cm, squares 20–30 cm, diamonds 30–40 cm, and open circles 40–50-cm depth.

3.2. Soil CO_2 concentrations and forest-floor CO_2 efflux

3.2.1. Seasonal and diurnal variations

Fig. 3 shows seasonal variations in soil CO_2 concentrations, forest-floor CO_2 efflux and storage in the 0–50 cm layer, soil temperature and soil water

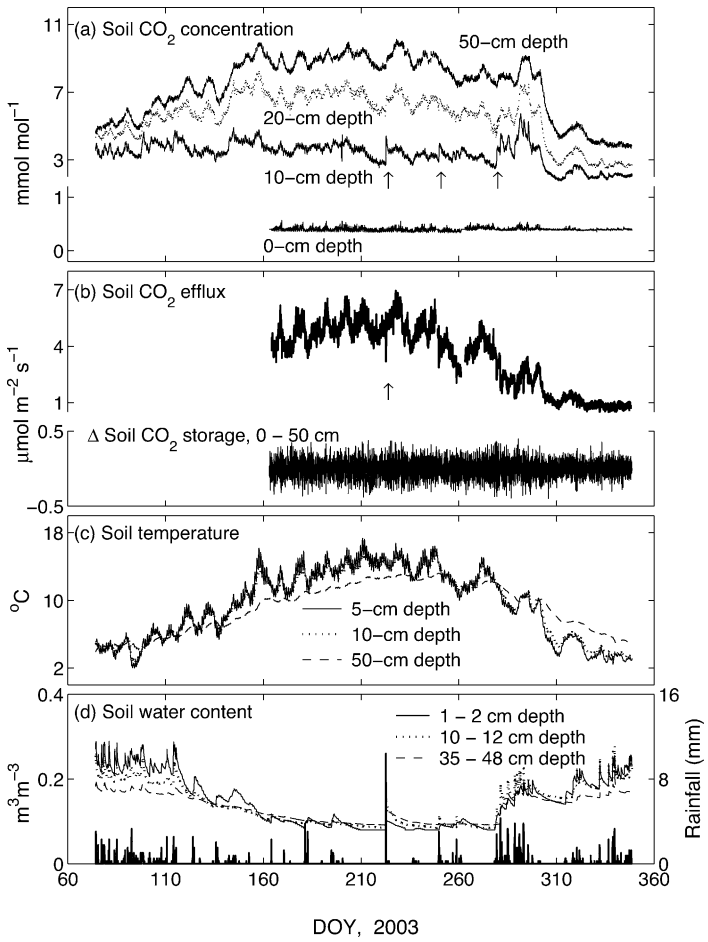

Fig. 3. Long-term time series of measured soil CO_2 concentration (a); soil CO_2 efflux and change in soil CO_2 storage (b); soil temperature (c); and soil water content and rainfall (d). Arrows indicate major rainfall event when the soil was initially relatively dry.

content at different depths. Seasonally, soil CO_2 concentrations as well as CO_2 efflux were well correlated with variations in soil temperature and soil water content. Soil CO_2 concentration also increased with soil depth reaching almost 10 mmol mol^{-1} at the 50-cm depth, which were higher than those measured with syringe sampling during 2000 (Jassal et al., 2004; Drewitt et al., 2005). Soil CO_2 efflux decreased from a summer high of 7.1 μmol m^{-2} s^{-1} to a winter low of 0.5 μmol m^{-2} s^{-1}. CO_2 concentration at ground level showed only small variation, and was related neither to CO_2 efflux nor to soil CO_2 concentrations. On an hourly basis, rates of change of CO_2 storage in the 0–50 cm soil layer were generally less than 0.2 μmol m^{-2} s^{-1}, occasionally approaching 0.4 μmol m^{-2} s^{-1}, some of which may be attributed to uncertainty in the measurements. The time rate of change of storage was an order of magnitude smaller than the measured efflux. Fig. 4 shows that diurnal maxima and minima of soil CO_2 concentration at the 10-cm depth as well as of CO_2 efflux coincided with maxima and minima of soil temperature at the 5-cm depth. Furthermore, time series analysis showed that soil CO_2 concentrations at all depths as well as soil CO_2 efflux varied in phase with each other and with soil temperature at the 5-cm depth. These results indicate the general occurrence of quasi steady-state conditions.

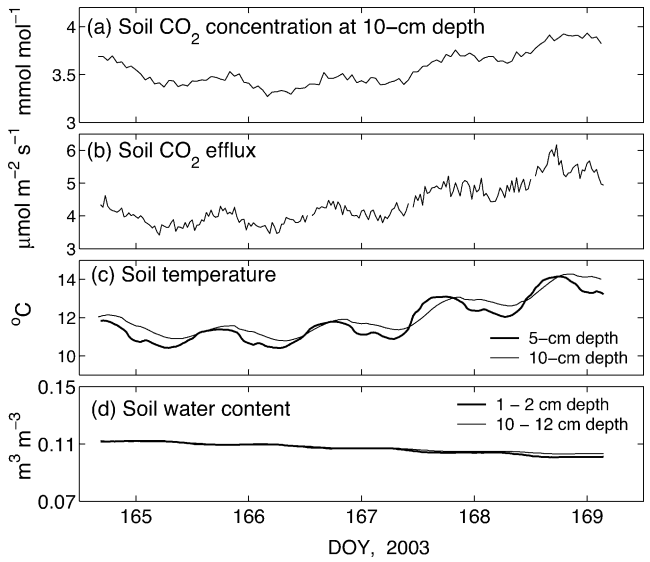

Fig. 4. Diurnal variation in soil CO_2 concentration (a) and soil CO_2 efflux (b) in relation to soil temperature (c) and soil water content (d).

The efflux was best described by an exponential function of soil temperature at the 5-cm depth:

$$F_e = F_{10} Q_{10}^{(T-10)/10} \quad (4)$$

with a reference efflux, F_{10} of 2.6 μmol m^{-2} s^{-1} and a Q_{10} of 3.7 and $R^2 = 0.98$. The temperature–efflux relationship showed seasonal hysteresis showing greater temperature sensitivity in the latter part of the year (Table 1), which can possibly be attributed to depletion of readily decomposable substrate (Kirschbaum, 2004). Such hysteresis-type behaviour in soil CO_2 effluxes has been also reported by Drewitt et al. (2002), Moren and Lindroth (2002) and Goulden et al. (1998). However, seasonal variations in labile carbon pools (Gu et al., 2004), plant phenological process (Yuste et al., 2004) and soil water content can significantly contribute to the seasonality of soil respiration, and, hence calculated Q_{10} values may not always represent true temperature sensitivity. When we excluded the data for the non-growing season (mean daily air temperature <6 °C), the seasonal differences in Q_{10} and F_{10} were much smaller with a mean Q_{10} of 2.5 (Table 1). We found a linear relationship between soil CO_2 concentration at the 50-cm depth and soil temperature at the 5-cm depth, with the data distinctly split into dry and warm, and wet and cool periods. The wet and cool period in this study corresponded to the non-growing season.

Table 1
Seasonal dependence of Q_{10} and F_{10} parameters in Eq. (4)

Period	Q_{10}	F_{10}	R^2
Rising soil temperatures	2.19	3.51	0.94
Falling soil temperatures (#)	3.89	2.56	0.98
	2.72	2.87	0.97
All (#)	3.74	2.60	0.98
	2.69	3.01	0.86
$\theta_{1-2} < 0.10$	2.49	3.11	0.88
$0.10 \leq \theta_{1-2} \leq 0.15$	2.49	3.11	0.88
$\theta_{1-2} > 0.15$ (#)	5.26	2.66	0.64
	2.59	2.47	0.71

Rising soil temperatures: from early June to end of July; falling soil temperatures: from early August to late-December; (#) excluding the non-growing season (mean daily air temperature ≤6 °C); θ_{1-2}: soil water content at the 1–2-cm depth.

Keeping in mind that the effects of soil water content on production and transport of CO_2 may influence the CO_2 efflux in opposite directions, relating the efflux to soil water content is not simple. Fig. 5a shows a weak negative correlation between efflux and soil water content at the 1–2-cm depth. However, this was probably because of the confounding effects of temperature and water content (Davidson et al., 1998) as a negative relationship between soil temperature and soil water content was observed. To isolate the effect of soil water content variation on the efflux, we normalized the effluxes by dividing the measured effluxes with those predicted with the best-

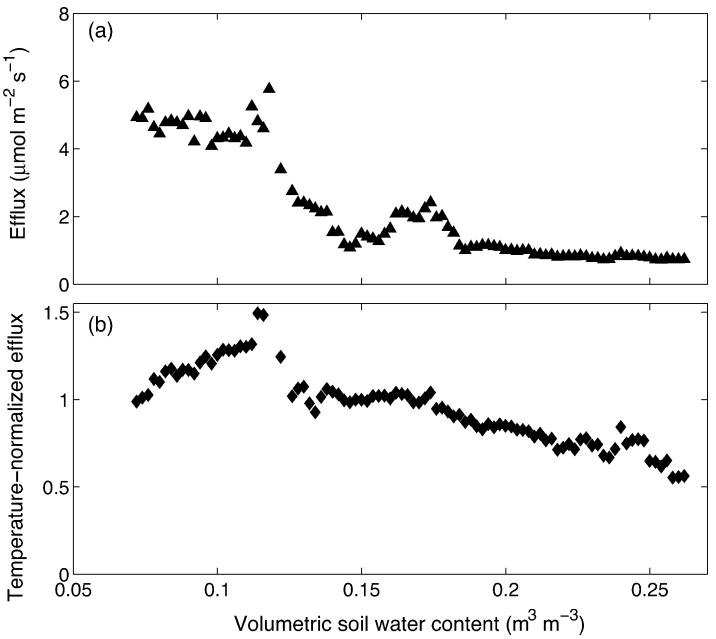

Fig. 5. Effect of soil water content at the 1–2-cm depth on measured soil CO_2 efflux (a); and the temperature-normalized efflux (b). The data are binned using bin widths of 0.0005 m^3 m^{-3} soil water content.

fit values of Eq. (4). This ratio of the temperature normalized efflux plotted against soil water content at the 1–2-cm depth (Fig. 5b) shows that the efflux increased with increase in soil water content up to about 0.12 m^3 m^{-3} and decreased with further increase in soil water content. These results are consistent with soil CO_2 efflux–water content relationships reported by many researchers (e.g. Bunnell et al., 1977; Hunt, 1977; vanVeen and Paul, 1981), especially Drewitt et al. (2002) at the site of the

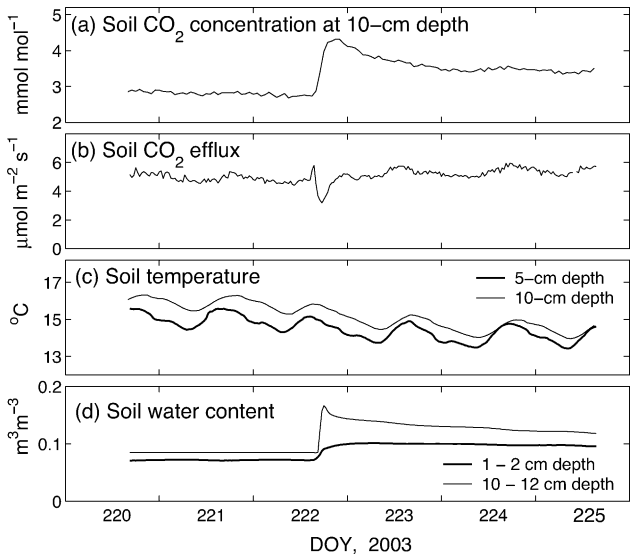

Fig. 6. As in Fig. 4 but before and after a major rainfall event when the soil was initially dry. See vertical arrows in Fig. 3.

present study. It is important to note the effect of major rain events, since following rain or sudden increases in soil water content, there can be appreciable increases in heterotrophic respiration or decreases in the diffusivity, which may influence the efflux as shown below.

3.2.2. *Influence of rainfall events*

Sudden increases in soil water content due to rain, especially when the soil was initially dry, resulted in significant increases in soil CO_2 concentrations (indicated by the arrows in Fig. 3a), particularly at shallow depths. For example, on DOY 222 (10 August), 12 mm of rain resulted in a large increase in CO_2 concentration at the 10-cm depth (Fig. 6a). Our measurements at this site during 2002 also showed similar effects of rain on soil CO_2 concentration at the 20-cm depth (Jassal et al., 2004). This phenomenon may be partly attributed to a decrease in diffusivity with increase in soil water content, and partly to the microbial flush (rapid increase in heterotrophic respiration) upon wetting a dry soil (Glinski and Stepniewski, 1985). However, immediately after rain the efflux decreased by about 40% (Fig. 6b) even though the CO_2 gradient across the 0–10 cm soil layer increased by 50%. Thus, the increased CO_2 concentration gradient was offset by the decrease in diffusivity so that the product of the two, i.e. the efflux, decreased. For this to occur, the mean diffusivity in the 0–10 cm layer should have decreased by more than 60% for a short period after rain. Calculations using mean soil water content in the top 10 cm layer showed that the diffusivity decreased from 2.4 $mm^2\ s^{-1}$ before rain to 1.2 $mm^2\ s^{-1}$ immediately after rain. Upon redistribution of soil water, the increase in mean soil water content of the 0–10 cm layer from 0.08 to 0.13 $m^3\ m^{-3}$ resulted in enhanced CO_2 production and the efflux increased by about 10% from its pre-rain values and stayed higher over the next few days despite a small decrease in soil temperature (Fig. 6c).

3.3. *Calculation of soil CO_2 flux distribution*

We used Eq. (2) to calculate the CO_2 flux distribution in the soil. This required the CO_2 diffusivity profiles that we calculated from measured soil water content and bulk density profiles using Eq. (3) with corrections for temperature effects using $D_T/D_{20} = [(273 + T)/298]^{1.75}$ (Campbell, 1985). Fig. 7a shows that in this well

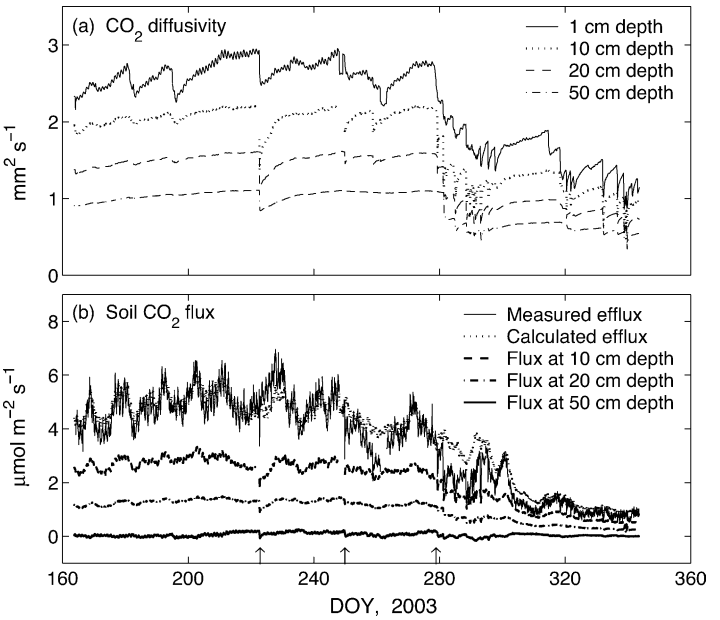

Fig. 7. (a) Time series of calculated soil CO_2 diffusivity at the surface and three depths and (b) CO_2 flux at the surface and the same three depths calculated using the concentration gradient method compared with chamber-measured soil CO_2 efflux. Arrows indicate major rain events.

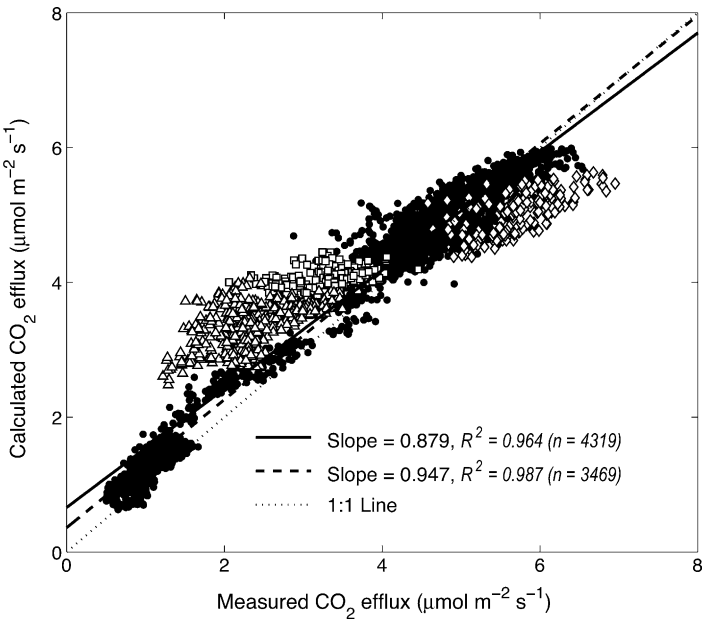

Fig. 8. Comparison of calculated and measured soil CO_2 effluxes shown in Fig. 9b. Triangles, squares and diamonds represent data ($n = 850$) for three episodes following major rainfall events indicated by arrows in Fig. 7b; solid circles ($n = 3469$) are the rest of the data. The thick lines are the linear least-squares best fits to the data with $n = 4319$: all data points, and $n = 3469$: solid circles only.

drained soil the diffusivity near the soil surface (calculated using Eq. (3) and soil characteristics at the 1-cm depth) exceeded that at lower depths during most of the year. To calculate soil CO_2 concentration gradients, we fitted a quadratic function of depth to CO_2 concentrations (Takle et al., 2004) at the 0, 10, 20 and 50-cm depths. To get robust estimates of concentration gradients at the 50-cm depth, we included estimated concentrations at the 100-cm depth obtained from seasonal ratios of concentrations at the 50-cm depth to those at the 100-cm depths obtained in previous studies at the site (Jassal et al., 2004; Drewitt et al., 2005). Drewitt et al. (2005) found that the vertical profiles of soil CO_2 generally had similar shapes throughout the year and between the consecutive years of 2000 and 2001.

Calculated CO_2 effluxes agreed well with measurements (Fig. 7b). Calculated CO_2 fluxes decreased with depth and were very small at the 50-cm depth, with more than 75% of the efflux originating in the top 20 cm soil layer. Fig. 7b also shows that following rainfall events, calculated effluxes were underestimated at low soil water contents and overestimated at high soil water contents (see Fig. 3d). Following significant rain events either measured soil water content at the 1–2-cm depth was not representative of the average water content near the surface resulting in poor estimates of the diffusivity, or the concentration gradients at the soil surface were not accurately estimated from quadratic fit to the concentrations. Not including the extrapolated concentration at the 1-m depth in the quadratic fit had almost no effect on the calculated effluxes and had a very small effect on fluxes at the 10- and 20-cm depths, but resulted in small downward fluxes at the 50-cm depth, likely due to artefacts of curve fitting. Fig. 8 compares measured with calculated soil CO_2 effluxes shown in Fig. 7b, indicating a tendency of slight overestimation for low to medium effluxes and slight underestimation for high effluxes.

We then used the gas transport equation for CO_2:

$$\frac{\partial(\varepsilon C)}{\partial t} = \frac{\partial}{\partial z}\left(D\frac{\partial C}{\partial z}\right) + S \tag{5}$$

to calculate S, the rate of soil CO_2 production (source strength, mol m^{-3} s^{-1}) profiles (Fig. 9). Similar to flux, the rate of production also decreased with depth, most of it concentrated in the top 20 cm soil layer and

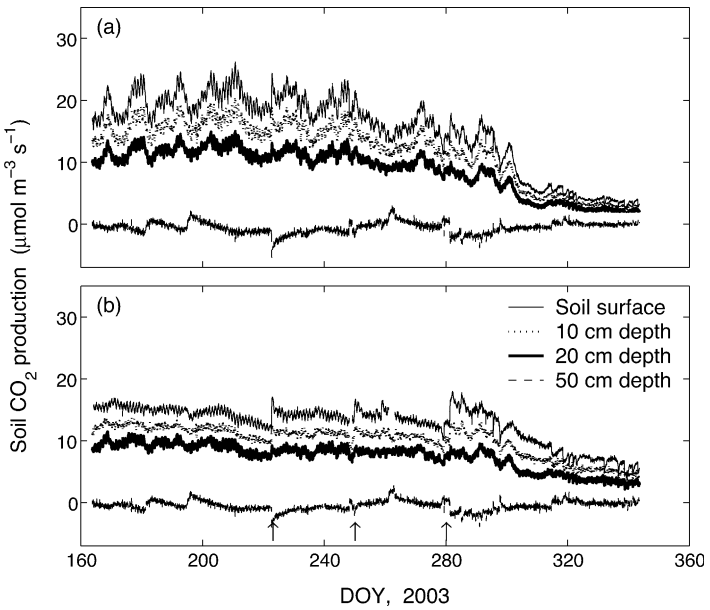

Fig. 9. Calculated time series of soil CO_2 production (a) and the same scaled to 10 °C using a Q_{10} of 2 for each layer (b). Arrows indicate major rain events.

approaching zero at the 50-cm depth. CO_2 production profiles scaled to 10 °C using a Q_{10} of 2 shows the sensitivity of production to changes in soil moisture due to rainfall episodes indicated by vertical arrows in Fig. 9b, particularly with the onset of the rainy season around DOY 280 when there was an appreciable increase in soil water content. The decline in CO_2 production in the top 20-cm soil layer after DOY 300 (25 October) was likely due to decreased root growth and the associated respiration at the end of the growing season. Fig. 9b also shows that small diurnal variations in CO_2 production persisted even after adjustment to a constant temperature, suggesting that other than soil temperature and water content some biological processes were influencing production on a smaller time scale.

Both the diffusivity (Fig. 7a) and the production (Fig. 9a) profiles were best described by a power function of soil depth, z (−ve below the soil surface), i.e. $D_0(-z - z_0)^m$ and $S_0(-z - z_0)^n$, respectively, where z_0 is a small value of z near the soil surface where D_0 and S_0 are measurable. Values of m and n varied from −0.29 to −0.17 and −0.62 to −0.46, respectively, though with no clear seasonal trend. Furthermore, it was found that $\partial(\varepsilon C)/\partial t$ was one to two orders of magnitude smaller than the flux divergence $(\partial(D\partial C/\partial z)/\partial z)$ at all depths, confirming that CO_2 production and transport in this soil was near steady-state.

3.4. Soil CO_2 efflux as a function of soil CO_2 concentration at a depth

That soil CO_2 was in quasi-steady-state suggests that soil CO_2 concentration at a selected depth may be used to estimate effluxes. We found that the efflux was linearly related to the CO_2 concentration at the 50-cm depth ($R^2 = 0.90$–0.96), with the slope varying with soil water content (Fig. 10). The R^2 decreased as soil depth decreased, most likely due to greater influence on soil CO_2 concentrations of short-term fluctuations in CO_2 diffusivity nearer the soil surface with rainfall events. The efflux at the same soil CO_2 concentration was lower and the slope of the efflux versus concentration line was smaller for wetter soil than for dry soil. These results are consistent with theory as can be shown from a steady-state ($\partial C/\partial t = 0$) solution of Eq. (5), with $D = D_0(-z - z_0)^m$ and $S = S_0(-z - z_0)^n$, subject to the boundary conditions:

$$\frac{\partial C}{\partial z} = 0, \qquad z = -L, \qquad t \geq 0 \tag{6}$$

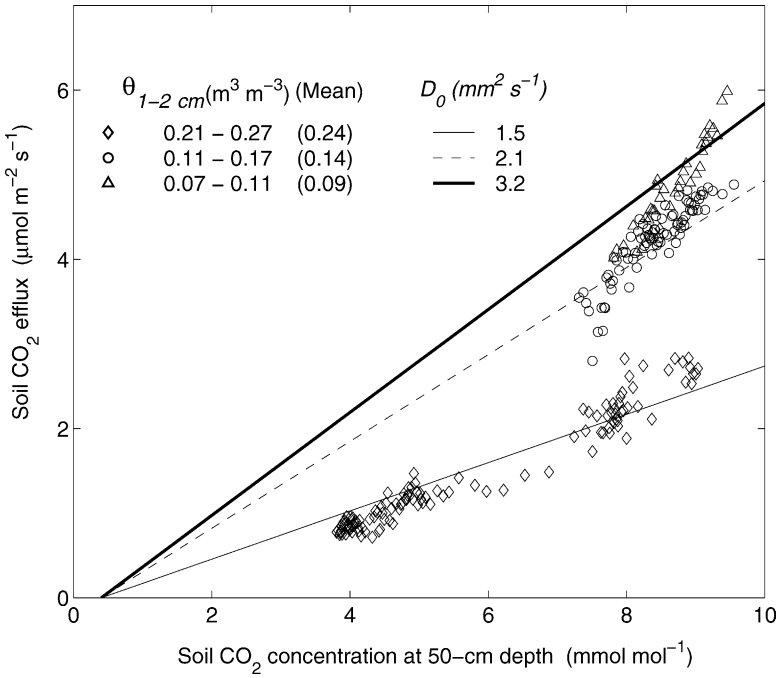

Fig. 10. Relationship between soil CO_2 efflux and soil CO_2 concentration at the 50-cm depth at different near-surface soil water contents. Lines are calculated using the steady-state model, Eq. (8) with $L = 2$ m, $m = -0.22$, $n = -0.54$, $C_0 = 0.4$ mmol mol^{-1}, and points are measured data classed according to indicated range of soil water content at the 1–2-cm depth. D_0 are diffusivities near the soil surface calculated using Eq. (3) with measured soil water contents at the 1–2-cm depth.

and

$$C = C_0, \qquad z = 0, \qquad t \geq 0 \tag{7}$$

which is

$$\frac{F_e}{D_0(C_z - C_0)} = -\left[\frac{(-z - z_0)^{n+2-m} - (-z_0)^{n+2-m}}{(n+2-m)L^{n+1}} - \frac{(-z - z_0)^{1-m} - (-z_0)^{1-m}}{1-m}\right]^{-1} \tag{8}$$

where L is the depth of an impermeable layer, C_0 is the CO_2 concentration at the soil surface, and $F_e = -D_0(\partial C/\partial z)_{z=0}$ is the soil CO_2 efflux. Fig. 10 also shows plots of F_e versus C_z calculated using Eq. (8) for representative D_0 values and with $z = 50$ cm; $C_0 = 0.40$ mmol mol^{-1}; $m = -0.22$, $n = -0.54$; $L = 2$ m. These results confirm that soil CO_2 was at steady-state most of the time, and show the possibility of using deep soil CO_2 concentration to estimate soil CO_2 efflux. The relatively large scatter of the measured data for very low soil water contents (0.07–0.11 m^3 m^{-3}) in summer may be due to: (a) a significant deviation of the diffusivity and the CO_2 production profile from the average power function ($m = -0.22$; $n = -0.54$) relationships with depth used in these calculations; (b) the diffusivity at the soil surface changing too fast to generate a single proportionality constant; (c) departure from steady-state conditions; and (d) presence of non-diffusive transport. We tested Eq. (8) by using it to calculate half-hourly soil CO_2 efflux during 2004 and comparing the results with effluxes measured using the automated soil chamber (Fig. 11). There was generally good agreement between the calculations and measurements except when the calculations were not able to reproduce the large fluctuations in measured effluxes during the summer.

4. Discussion

We found that soil CO_2 concentrations at all depths and soil temperature at the 5-cm depth varied in phase diurnally as well as seasonally. Hirsch et al. (2002)

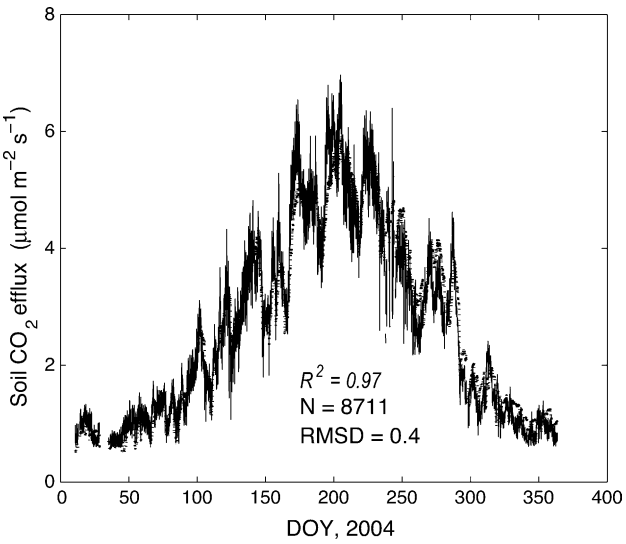

Fig. 11. Comparison of time series of chamber measured soil CO_2 effluxes (solid line) and those calculated using the steady-state diffusion model, Eq. (8) (dotted line). *N*: number of samples; RMSD: root mean square difference ($\mu mol\ m^{-2}\ s^{-1}$).

studied deep (>20-cm depth) soil CO_2 concentration following thaw in a mature boreal forest and found that the seasonal pattern of daily mean soil CO_2 concentration and soil temperature at depths up to 23 cm were in phase, but diurnal cycles of CO_2 concentration and soil temperature were not in phase. The latter was explained as an effect of air turbulence at the soil surface causing CO_2 to be released from the soil in the morning when the wind speed increased, and to accumulate in the soil when the wind speed dropped in the evening. Our measurements did not show such behaviour possibly because of high soil CO_2 diffusivity and because wind speed does not vary much near the forest floor at this site with a dense canopy (Drewitt, 2002).

Response of soil respiration to rain can be viewed in terms of: (a) increased production of CO_2 in the soil due to enhanced microbial activity; (b) decreased diffusivity due to decrease in air-filled pore space; and (c) displacement of CO_2-rich soil air by rain water. Many studies in different forest ecosystems (e.g. Borken et al., 2003; Yuste et al., 2004; Irvine and Law, 2002; Lee et al., 2002) have reported that when the soil was dry, even a small rainfall event, which only slightly increased the water content in mineral soil, had resulted in a significant increase in soil CO_2 efflux. Lee et al. (2004) studied the impact of artificial wetting through simulated rain in isolated 1-m radius plots in a mixed forest. They reported an instant increase in CO_2 efflux when water was sprayed over the forest floor with the efflux returning to its pre-irrigation values in less than 1 h after the irrigation, and showed no post-wetting respiration pulse. The instant increase in the efflux upon small wetting events was attributed to the decomposition of active carbon compounds in the litter layer (Borken et al., 2003; Lee et al., 2004). In comparison, the efflux decreased immediately after rain and recovered to pre-irrigation or even somewhat higher value in 2 h after the irrigation when litter layer had been removed prior to the experiment (Lee et al., 2004). Yang (1998) observed enhanced CO_2 efflux during rainfall events in an old aspen forest and attributed it mainly to displacement of CO_2-enriched soil air. We found that soil CO_2 efflux decreased immediately after major rain events, especially when the soil was dry, because of decreased diffusivity, but recovered soon after and within hours surpassed the pre-rain value presumably due to increased microbial activity. Since there was no instant increase in CO_2 efflux as a result of rain, displacement of CO_2-rich soil air is ruled out. Ball et al. (1999) reported that periods of low or zero CO_2 efflux under no-tillage in an agricultural field caused by heavy rainfall were associated with reduced gas diffusivity.

Many researchers (e.g. Rayment and Jarvis, 2000; Anthoni et al., 2004) emphasize the importance of considering soil CO_2 storage to correct fluxes measured

with eddy covariance technique. Anthoni et al. (2004), considering a change in CO_2 concentration in the 0–30 cm soil of 100 μmol mol^{-1} over a half-hour, reported a change in CO_2 storage of 0.7 μmol m^{-2} s^{-1}, −1, though they seem to have used total porosity rather than air-filled porosity in their calculations. With an air-filled porosity of 0.3, this change in CO_2 storage would be 0.2 μmol m^{-2} s^{-1}. Drewitt et al. (2005), working at the same site as in the present study, reported that over a period of 28 h, CO_2 concentration in the top 10 cm layer showed only 4% deviation from the mean, which was about the same as the uncertainty in measurements. Our results showed that soil CO_2 storage flux was generally small, at least an order of magnitude smaller than the measured efflux, and was not related to friction velocity (u_*). Furthermore, these results, along with the observation that soil CO_2 efflux and concentration at all the three depths and shallow depth soil temperatures varied in phase, suggest that the steady-state assumption was reasonable.

Tang et al. (2003), using solid-state CO_2 sensors in a Mediterranean savanna ecosystem, reported that the effluxes calculated from concentration gradients, were 9% underestimated compared to measurements when diffusivities were obtained from the Millington–Quirk model, but were 18% overestimated when the Marshall model was used to obtain diffusivities. Liang et al. (2004) found that CO_2 effluxes estimated from soil CO_2 gradients, using measured diffusivities, were systematically higher by 45% than measured with automated and open-top chamber systems. They further reported that under non-steady-state conditions in the field, CO_2 effluxes estimated from concentration gradients did not correlate well with the LI-6400-09 soil chamber measurements. Potential sources of error in the gradient technique include: (a) difficulty in obtaining an accurate estimate of diffusivity either from models or by measurement; (b) difficulty in correctly estimating the soil CO_2 concentration gradient near the soil surface. Our results showed that effluxes calculated from soil CO_2 concentration gradients were very similar to the measured values, except following major rainfall events when they were underestimated at low soil water contents and overestimated at high soil water contents. Furthermore, steady-state conditions occurred for most of the time and efflux was significantly correlated with soil CO_2 concentration at the 50-cm depth. Relating efflux to soil CO_2 concentration is simple and does not suffer from the above-mentioned errors. This method shows promise as the deep soil CO_2 concentration is expected to show less spatial variation than chamber-measured effluxes due to uneven distribution of organic substrate near the soil surface (Drewitt et al., 2002; Rayment and Jarvis, 2000). We recommend that future investigations should focus on determining the spatial variability of deep soil CO_2 concentrations under different soil and environmental conditions.

5. Conclusions

1. A simple steady-state method of measuring CO_2 diffusivity in undisturbed soil cores is described. The method accounts for CO_2 production in the soil and uses an analytical solution to the diffusion equation. The diffusivity was related to air-filled porosity with a power law function, which was independent of soil depth.
2. Effluxes calculated from near-surface concentration gradients and diffusivities agreed well with chamber-measured effluxes.
3. Calculations showed that more than 75% of the CO_2 efflux originated at depths shallower than 20 cm.
4. In-phase diurnal and seasonal variations in soil CO_2 efflux, concentrations and shallow depth soil temperature, and negligible rates of change in soil CO_2 storage showed that CO_2 production and transport in this soil were generally at steady-state.
5. As there was no instant increase in CO_2 efflux as a result of rain, displacement of CO_2-rich soil air by rain in this soil is ruled out.
6. Soil CO_2 efflux was best described by a linear function of CO_2 concentration at the 50-cm depth with the slope being a function of soil water content, which was consistent with a simple steady-state model. Calculated effluxes using soil CO_2 concentrations at the 50-cm depth and soil water content in the 1–2 cm layer were very close to the chamber-measured effluxes during 2004.

Acknowledgements

This research was funded by the Canadian Foundation for Climate and Atmospheric Sciences

(CFCAS) as a part of Development of a Canadian Global Coupled Carbon Climate model (GC^3M) project, a Natural Sciences and Engineering Research Council (NSERC) operating grant, and the Fluxnet Canada Research Network. We thank Andrew Sauter and Rick Ketler for field and laboratory work support during the course of this research.

Appendix A

Under steady-state conditions, the diffusion equation is:

$$\frac{\partial F}{\partial z} = S \tag{A.1}$$

where $F = -D\partial C/\partial z$ is the flux (μmol m^{-2} s^{-1}) positive upwards, S is the rate of CO_2 production (+ve) in the soil (μmol m^{-3} s^{-1}) and z is soil depth (m) negative downwards. Assuming S is constant over the vertical extent of the soil column, the solution to Eq. (A.1) subject to the boundary conditions:

$$C = C_0, \qquad z = 0 \tag{A.2}$$

and

$$C = C_L, \qquad z = -L \tag{A.3}$$

is:

$$D = \frac{L(F_0 + F_L)/2}{C_L - C_0} \tag{A.4}$$

where F_0 and F_L are the fluxes at the soil surface and at the bottom of the column at $z = -L$ ($L = 10$ cm in Fig. 1), respectively, with C_0 and C_L as the respective soil CO_2 concentrations (μmol m^{-3}). Substituting $F_0 - F_S$ for F_L, where F_S (+ve) is the total CO_2 production in the soil column of length L (i.e. LS), in Eq. (A.4), gives the following expression for calculating D in the steady-state soil column measurements:

$$D = \frac{L(F_0 - F_S/2)}{C_L - C_0} \tag{A.5}$$

References

Anthoni, P.M., Friebauer, A., Kolle, O., Schulze, E.D., 2004. Winter wheat carbon exchange in Thuringia. Germany. Agric. For. Meteorol. 121, 55–67.

Ball, B.C., Scott, A., Parker, J.P., 1999. Field N_2O, CO_2 and CH_4 fluxes in relation to tillage, compaction and soil quality in Scotland. Soil Till. Res. 53, 29–39.

Borken, W., Davidson, E.A., Savage, K., Gaudinski, J., Trumbore, S.E., 2003. Drying and wetting effects on carbon dioxide release from organic horizons. Soil Sci. Soc. Am. J. 67, 1888–1896.

Bunnell, F.L., Tait, D.E.N., Flanagan, P.W., vanCleve, K., 1977. Microbial respiration and substrate weight loss. I. A general model of the influence of abiotic variables. Soil Biol. Biochem. 9, 33–40.

Campbell, G.S., 1985. Soil Physics with BASIC. Springer-Verlag, New York, 150 pp.

Currie, J.A., 1965. Diffusion within the soil microstructure—a structural parameter for soils. J. Soil Sci. 16, 279–289.

Davidson, E.A., Delc, E., Boone, R.D., 1998. Soil water content and temperature as independent or confounded factors controlling soil respiration in a temperate mixed hardwood forest. Global Change Biol. 4, 217–227.

Davidson, E.A., Trumbore, S.E., 1995. Gas diffusivity and production of CO_2 in deep soils of the eastern Amazon. Tellus 47B, 550–565.

Drewitt, G.B. 2002. Carbon dioxide flux measurements from a coastal Douglas-fir forest. Unpublished Ph.D. thesis, University of British Columbia, Vancouver, BC.

Drewitt, G.B., Black, T.A., Jassal, R.S., 2005. Using measurements of soil CO_2 efflux and concentrations to infer the depth distribution of CO_2 production in a forest soil. Can. J. Soil Sci. 85, in press.

Drewitt, G.B., Black, T.A., Nesic, Z., Humphreys, E.R., Jork, E.M., Swanson, R., Ethier, G.J., Griffis, T., Morgenstern, K., 2002. Measuring forest floor CO_2 fluxes in a Douglas-fir forest. Agric. For. Meteorol. 110, 299–317.

Eswaran, H., van den Berg, E., Reich, P., 1993. Organic carbon in soils of the world. Soil Sci. Soc. Am. J. 57, 192–194.

Fang, C., Moncrieff, J.B., 1998. A simple and fast technique for measuring the CO_2 profile in the soil. Soil Biol. Biochem. 30, 2107–2112.

Fang, C., Moncrieff, J.B., 1999. A model of CO_2 production and transport. 1. Model development. Agric. For. Meteorol. 95, 225–236.

Glinski, J., Stepniewski, W., 1985. Soil Aeration and its Role for Plants. CRC Press, Boca Raton, FL, USA, 229 pp.

Goulden, M.L., Crill, P.M., 1997. Automated measurement of soil CO_2 exchange at the moss surface of a black spruce forest. Tree Phyiol. 17, 537–542.

Goulden, M.L., Wofsy, S.C., Harden, J.W., Trumbore, S.E., Crill, P.M., Gower, S.T., Fries, T., Daube, B.C., Fan, S.M., Sutton, D.J., Bazzaz, A., Munger, J.W., 1998. Sensitivity of boreal forest carbon balance to soil thaw. Science 279, 214–217.

Gu, L., Post, W.M., King, A.W., 2004. Fast labile carbon turnover obscures sensitivity of heterotrophic respiration from soil to temperature: a model analysis. Global Biogeochem. Cycles 18: GB1022, doi: 10.1029/2003GB002119.

Hirsch, A.I., Trumbore, S.E., Goulden, M., 2002. Direct measurement of the deep soil respiration accompanying seasonal thawing of a boreal forest soil. J. Geophys. Res. 108, 11–20.

Houghton, J.T., Meira Filho, L.G., Bruce, J., 1995. Climate change. In: In Radiative Forcing of Climate Change and an Evaluation of

the IPCC's 92 Emission Scenariosunknown:book, Cambridge University Press, Cambridge, UK.

Hunt, H.W., 1977. A simulation model for decomposition for grasslands. Ecology 58, 469–484.

Irvine, J., Law, B.E., 2002. Contrasting soil respiration in young and old growth ponderosa pine forests. Global Change Biol. 8, 1183–1194.

Janssens, I.A., Matteucci, H.G., Kowalski, A.S., Buchman, N., Epron, D., Pilegaard, K., Kutsch, W., Longdoz, B., Grunwald, T., Montagnani, L., Dore, S., Rebmann, C., Moors, E.J., Grelle, A., Rannik, U., Morgenstern, K., Oltchev, S., Clement, R., Gudmundsson, J., Minerbi, S., Berbigier, P., Ibrom, A., Moncrieff, J., Aubinet, M., Bernhofer, C., Jensen, N.O., Vesala, T., Granier, A., Schulze, E.D., Lindroth, A., Dolman, A.J., Jarvis, P.G., Ceulamans, R., Valentini, R., 2001. Productivity overshadows temperature in determining soil and ecosystem respiration across European forests. Global Change Biol. 7, 269–278.

Jassal, R.S., Black, T.A., Drewitt, G.B., Novak, M.D., Gaumont-Guay, D., Nesic, Z., 2004. A model of the production and transport of CO_2 in soil: predicting soil CO_2 concentrations and CO_2 efflux from a forest floor. Agric. For. Meteorol. 124, 219–236.

Jury, W.A., Gardner, W.R., Gardner, W.H., 1991. Soil Physics. Wiley, New York, 328 pp.

Kanemasu, E.T., Powers, W.L., Sij, J.W., 1974. Field chamber measurements of CO_2 flux from soil surface. Soil Sci. 118, 233–237.

Kirschbaum, M.U.F., 2004. Soil respiration under prolonged soil warming: are rate reductions caused by acclimation or substrate loss? Global Change Biol. 10, 1–8.

Law, B.E., Ryan, M.G., Anthoni, P.M., 1999. Seasonal and annual respiration of a Ponderosa pine ecosystem. Global Change Biol. 5, 169–182.

Lee, M.S., Nakane, K., Nakatsubo, T., Mo, W.H., Koizumi, H., 2002. Effects of rainfall events on soil CO_2 flux in a cool temperate deciduous broad-leaved forest. Ecol. Res. 17, 401–409.

Lee, X., Wu, H.J., Singler, J., Oishi, C., Siccama, T., 2004. Rapid and transient response of soil respiration to rain. Global Change Biol. 10, 1017–1026.

Liang, N., Nakadai, T., Hirano, T., Qu, L., Koike, T., Fujinuma, Y., Inoue, G., 2004. In situ comparison of four approaches to estimating soil CO_2 efflux in a northern larch (*Larix kaempferi Sarg.*) forest. Agric. For. Meteorol. 123, 97–117.

Marshall, T.J., 1959. The diffusion of gas through porous media. J. Soil Sci. 10, 79–82.

Millington, R.J., 1959. Gas diffusion in porous media. Science 130, 100–102.

Millington, R.J., Quirk, J.P., 1961. Permeability of porous solids. Trans. Faraday Soc. 57, 1–8.

Moldrup, P., Olsen, T., Yamaguchi, T., Schjonning, P., Rolston, D.E., 1999. Modelling diffusion and reaction in soil. IX. The Buckingham–Burdine–Campbell equation for gas diffusivity in undisturbed soil. Soil Sci. 164, 542–551.

Moren, A.S., Lindroth, B.A., 2002. CO_2 exchange at the floor of a boreal forest. Agric. For. Meteorol. 101, 1–14.

Penman, H.L., 1940. Gas and vapour movement in the soil. I. The diffusion of vapours through porous solids. II. The diffusion of carbon dioxide through porous solids. J. Agric. Sci. 30, 437–462, 570–581.

Petersen, L.W., Rolston, D.E., Moldrup, P., Yamaguchi, T., 1994. Volatile organic vapour diffusion and adsorption in soils. J. Environ. Qual. 23, 799–805.

Rayment, M.B., Jarvis, P.G., 2000. Temporal and spatial variation of soil CO_2 efflux in a Canadian boreal forest. Soil Biol. Biochem. 32, 35–45.

Rolston, D.E., 1986. Gas diffusivity. In: Methods of Soil Analysis. Part 1. Physical and Mineralogical Methodsunknown:book, ASA, Madison, USA, pp. 1089–1119.

Sallam, A., Jury, W.A., Letey, J., 1984. Measurement of gas diffusion coefficient under relatively low air-filled porosity. Soil Sci. Soc. Am. J. 48, 3–6.

Schimel, D.S., 1995. Terrestrial ecosystems and carbon cycle. Global Change Biol. 1, 77–91.

Schlesinger, W.H., Andrews, J.A., 2000. Soil respiration and the global carbon cycle. Biogeochem. 48, 7–20.

Simunek, J., Saurez, D.L., 1993. Modelling carbon dioxide transport and production in soil. 1. Model development. Water Resour. Res. 29, 487–497.

Takle, E.S., Massman, W.J., Brandle, J.R., Schmidt, R.A., Zhou, X., Litvina, I.V., Garcia, R., Doyle, G., Rice, C.W., 2004. Influence of high-frequency ambient pressure pumping on carbon dioxide efflux from soil. Agric. For. Meteorol. 124, 193–206.

Tang, J., Baldocchi, D.D., Qi, Y., Xu, L., 2003. Assessing soil CO_2 efflux using continuous measurements of CO_2 profiles in soils with small solid-state sensors. Agric. For. Meteorol. 118, 207–220.

vanVeen, J.A., Paul, E.A., 1981. Organic carbon dynamics in grassland soils. I. Background information and computer simulation. Can. J. Soil Sci. 61, 185–201.

Welles, J.M., Demetriades-Shah, T.H., McDermitt, D.K., 2001. Considerations for measuring ground CO_2 effluxes with chambers. Chem. Geol. 177, 3–13.

Widen, B., Lindroth, A., 2003. A calibration system for soil carbon dioxide efflux measurement chambers: description and application. Soil Sci. Soc. Am. J. 67, 327–334.

Yang, P.C., 1998. Carbon dioxide flux within and above a boreal aspen forest. Unpublished Ph.D. thesis, University of British Columbia, Vancouver.

Yuste, J.C., Janssens, I.A., Carrara, A., Ceulemans, R., 2004. Annual Q_{10} of soil respiration reflects plant phonological patterns as well as temperature sensitivity. Global Change Biol. 10, 161–169.